New insights on post-myocardial infarction ventricular tachycardia ablation: defining patient-tailored endpoints to improve outcome

De Riva Silva, M.

Part I

2

Twelve-lead ECG of ventricular tachycardia in structural heart disease

Marta De Riva, MD, Masaya Watanabe, MD, PhD, Katja Zeppenfeld, MD, PhD

Circulation: Arrhythmia & Electrophysiology 2015;8(4):951-962

INTRODUCTION

In patients with structural heart disease (SHD), defined by the presence of myocardial scarring either on cardiac imaging and/or electroanatomical (EAM) mapping, catheter ablation is increasingly employed for the treatment of ventricular tachycardia (VT).

With more detailed knowledge of potential substrates and anatomical structures involved in VT, not only the endocardium of the left (LV) and right ventricle (RV) but also more complex structures like the aortic root, the cardiac veins or the epicardium have become areas of interest for ablation.

Pre-procedural analysis of the clinically documented VT 12-lead electrocardiogram (ECG) is often used to predict the *VT site of origin* (SoO) and it is considered to be an important tool for planning the ablation, to estimate the probability of success and to recognize potential procedural limitations and related risks. These factors may have important implications for patient advice and decision making but also for the selection of a center capable to perform the expected procedure.

Since the majority of inducible VTs in patients with SHD are not hemodynamically tolerated[1-2], a detailed analysis of the VT 12-lead ECG of each induced VT may also be helpful. Combining the ECG with information of the scar size and distribution obtained from EAM during sinus rhythm or from pre-procedural imaging may direct mapping to the area of interest with the potential of increasing procedural success and to reduce procedural duration.

In this review we will focus on the reported evidence for the value of the 12-lead VT ECG as a "mapping tool" in patients with scar related VT and discuss its potential implications when combined with scar information from EAM or imaging.

VENTRICULAR TACHYCARDIA SITE OF ORIGIN

The mechanism of the majority of VTs in patients with structurally normal hearts is focal, and the 12-lead ECG can be very helpful to predict its SoO, since rapid activation of the normal myocardium from a focal source results in typical QRS patterns[3].

As a general rule, VTs originating from the structurally normal LV have a right bundle branch block (RBBB) morphology (defined as predominant R in lead V1) and VTs from the normal RV have a left bundle branch block (LBBB) morphology (defined as predomi-

nant S in lead V1). The precordial transition for RBBB VTs (first lead with a predominant S) changes from positive concordant for VTs originating from the base of the LV to progressively earlier transition in V2-V4 as the VT origin moves towards the apex of the ventricle. For LBBB VTs, VTs originating from the basoseptal area of the RV have an early transition (first lead with a predominant R) and the transition becomes progressively later as the VT origin moves towards the ventricular free wall. With regard to the frontal plane axis, VTs originating from the superior aspect of the ventricles show an inferior axis (predominant R in aVF), VTs from the inferior aspect of the ventricles a superior axis (predominant S in aVF), LV free wall VTs have typically a right axis (with a dominant S in I and aVL) and septal VTs typically a left axis (with a dominant R in I and aVL). Finally, septal VTs have a narrower QRS than VTs from the ventricular free wall.

In contrast to patients with structurally normal hearts, the majority of VTs in patients with SHD are due to scar related reentry. The SoO of a scar related reentrant VT has been differently defined as 1) the *"VT exit site"*, from which the *normal* myocardium is rapidly activated which corresponds to the scar border and coincides with the QRS onset on the surface ECG [4-7]; 2) the *"reentry circuit exit site"* from which the activation wavefront emerges from the critical slow conducting VT isthmus which may not necessarily correspond with the scar border and may precede the activation of the rapidly conducting myocardium with only little effect on the 12-lead ECG or 3) *'the target site for ablation"*, usually defined as the critical slow conducting VT isthmus, which is activated during diastole, thereby not contributing to the surface ECG at all[8]**.**

Figure 1.

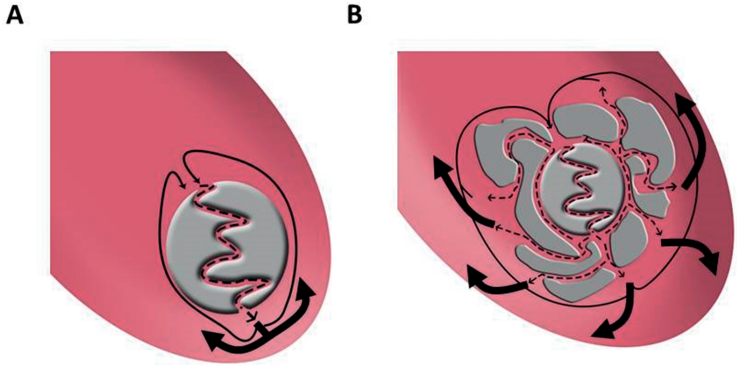

Panel A: Schematic representation of a VT reentry circuit. The reentry circuit exit site corresponds with the scar border zone. Rapid activation (indicated by large arrows) of the normal myocardium determines the VT QRS morphology. Pacing at the scar exit site will likely resemble the VT morphology.
Panel B: Schematic representation of a complex scar with one potential VT reentry circuit. The reentry circuit is located within the scar. The wave front emerges from the exit of the reentry circuit isthmus and propagates through multiple small pathways activating the remaining normal myocardium from different sites giving rise to a "fused" QRS complex. In this case, the VT morphology may not help to predict the scar exit site.

The 12-lead ECG morphology of a scar related reentrant VT depends mainly on the VT exit site, or the site(s) or the area(s) from which the normal myocardium is activated. Thus, only if the reentry circuit exit site coincides with the scar border, the 12-lead VT ECG may be helpful to directly guide to the area of interest for ablation **(Figure 1, see supplement Case 1)**.

Furthermore, the overall size and distribution of the scar and the size, distribution and properties of the remote myocardium determine the overall 12-lead VT ECG morphology. Therefore, in patients with large scars, the accuracy of the 12-lead ECG to localize the VT SoO may be limited also for tachycardias with a focal mechanism.

VALUE OF THE 12-LEAD ECG TO PREDICT THE ENDOCARDIAL VT SITE OF ORIGIN IN PATIENTS WITH PRIOR MYOCARDIAL INFARCTION

Site of origin as "exit site"

In the pioneering work of Miller et al.[4], the VT SoO was defined as the *earliest recorded activity on the second half of the diastole during endocardial VT activation mapping*. All 182 mapped VTs from 102 patients with single prior myocardial infarction (MI) had one endocardial site activated at least *40ms before the QRS onset*. Each 12 lead ECG of VT was categorized according to the location of the MI (anterior or inferior), the bundle branch block (BBB) type configuration, the frontal plane axis and one of 8 prespecified precordial R-wave progression patterns **(Figure 2A)**. A specific morphology of VT was defined as a characteristic morphology (based on the combination of these 4 factors) that was associated with one of 11 predefined LV regions based on fluoroscopy with a positive predictive value (PPV) greater than 70% **(Figure 2B).**

Of the 128 VTs in 73 patients with anterior MI, only 47 (37%) had such a specific morphology. Fifty VTs (39%) had a LBBB morphology, suggesting a septal VT exit site. Among the LBBB VTs, 37 (74%) had one of two identified specific patterns: 90% of the VTs with a left superior axis and a late or no transition were mapped to the inferoapical septum and the majority of VTs (81%) with inferior axis regardless of the precordial pattern were mapped to the anteroapical septum **(see supplement, Case 2).** Of the 78 VTs (61%) with a RBBB morphology, only 10 (13%) had a specific morphology: 7 out of 10 VTs (70%) which had a right inferior axis and either dominant or abrupt loss precordial pattern was also related to the anteroapical septum **(Figure 2C).**

Figure 2.

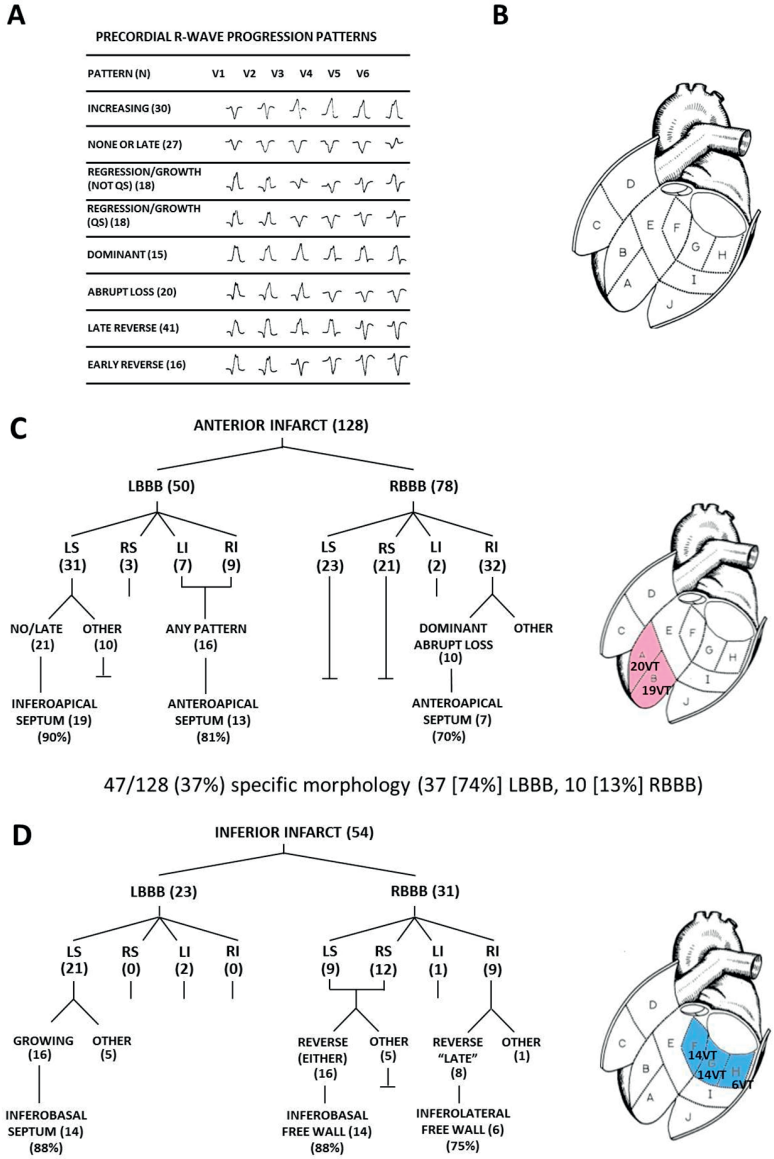

Algorithm proposed by Miller et al.[4] to predict the endocardial VT site of origin based on the 12-lead ECG VT morphology including BBB, axis and precordial transition pattern (Panel A) according to a 11 LV regions model (Panel B) in patients with anterior (Panel C) and inferior (Panel D) myocardial infarction. (Modified from Miller et al., Circulation 1988)

Regions of VT origin: A, inferoapical septum; B, anteroapical septum; C, anteroapical free wall; D, anterobasal free wall; E, anterobasal and mid septum; F, inferobasal septum; G, inferomedial free wall; H, inferolateral free wall; I, midinferior wall; J, inferoapical free wall; regions G and H together are the inferobasal free wall.

LBBB indicates left bundle branch block; RBBB, right bundle branch block; LS, left superior axis; RS, right superior axis; LI, left inferior axis; RI, right inferior axis.

For inferior MI the results were better. In 40 out of 54 VTs (73%) from 35 patients, a specific morphology could be identified. Of the 23 VTs (43%) with LBBB morphology, 88% of those with left superior axis and a growing precordial pattern were mapped to the inferobasal septum. Thirty-one VTs had RBBB morphology (57%) and of them, two specific morphologies could be determined: 14 out of 16 VTs (88%) with superior axis and either an early or late reverse precordial pattern were mapped to the inferobasal free wall whereas 8 out of 9 VTs (75%) **(see supplement, Case 3)**, with right inferior axis and a late reverse precordial pattern were mapped to the inferolateral wall **(Figure 2D).**

In this paper, an association between a specific 12-lead ECG VT morphology and one of the 11 predefined LV regions could only be found for 48% of the mapped VTs. Specific morphologies were more often identified in patients with inferior infarction and for VTs with LBBB morphology. In patients with anterior MI, only apicoseptal exit sites could be correctly identified.

The algorithm was developed before the advent of EAM and delayed enhancement MRI (DE-MRI) to delineate scar. Accordingly, it could not correct for variations in anterior and lateral scar extension which may explain the lack of additional identified specific patterns, in particular for RBBB VTs after anterior MI **(see supplement, Cases 4 and 5).** In contrast, scar extension in inferior MI may be less variable, as these scars are often restricted to the basal inferoseptal and posterior regions with the mitral annulus as one common boundary. The limited mapping density, with on average 9 catheter positions using a catheter with a 1cm tip electrode and an interelectrode spacing of 5 mm may have also reduced the accuracy of the algorithm. The broad definition of a VT exit site applied in this study may encompass VT exit sites from the scar border zone, VT reentrant circuit exit sites but also critical isthmus sites, which may further influence the predictive value of the algorithm for a specific location. Of note, the RV as potential site of origin was not included, which may contain reentry circuit and scar exit sites **(see supplement, Case 2)**

Based on the assumption that pacing at the VT endocardial exit site may generate a QRS morphology identical to the VT morphology, Kuchar et al.[5] proposed a different algorithm for localizing the VT SoO. They used ventricular pace-mapping as surrogate for a VT exit site. Ninety-three 12-lead ECGs recorded during pacing from different sites in 22 patients with single or multiple prior MI were analyzed and correlated to one of 24 LV regions based on fluoroscopy. Five paced QRS complex features could be related or were exclusive for a particular region:

1) A negative QRS in *precordial lead V1* was typical for septal sites, but never observed during pacing at lateral LV sites.

2) The QRS in *precordial lead V4* was never negative by pacing at the basal LV and never positive when pacing at apical regions.
3) A positive QRS in *lead I* was never observed when pacing from the lateral LV.
4) A predominant negative QRS in *lead aVL* was observed when pacing from the lateral LV and a predominant positive QRS in lead aVL when pacing from the septum.
5) A positive QRS in *lead II* was never observed during pacing from inferior sites.

From these data an algorithm was derived and subsequently tested in 44 induced VTs from 42 additional patients in which the VT SoO could be determined by activation mapping **(Figure 3)**. Precise localization of the endocardial VT exit site using this algorithm was only possible for 39% of the VTs. The algorithm showed a high accuracy (80-90%) to distinguish between anterior, inferior, septal and lateral LV regions but was not useful to predict central and midventricular sites and only moderately successful in differentiating sites in the long axis of the ventricle (e.g. basal vs apical) (55-70%).

As for Miller's algorithm, the size and extension of the scar may significantly influence the accuracy of the algorithm to predict the VT SoO. Moreover, pacing at the scar border zone and at potential critical isthmus sites within the scar may not necessarily result in the same 12-lead ECG morphology with different stimulus to QRS intervals than the VT ECG. In particular for small scars, activation patterns during pacing may be different from the propagation during VT since reentry circuits may also be determined by areas of functional block only present during VT. In these cases a 12/12 lead pace-match of the VT ECG cannot be achieved. For large scars, De Chillou et al.[9] could recently demonstrate that the best match between the paced QRS morphology and the VT morphology could be obtained if pacing was performed at the VT exit region or towards the exit part of the critical VT isthmus. In contrast, pacing at the VT entrance region or at the entrance part of the critical VT isthmus resulted in a completely different QRS complex morphology due to the activation of the preserved myocardium in the opposite direction than during VT. Despite this limitation, careful comparison of the paced ECG morphologies with the VT ECG may still be very useful to determine the area of interest if combined with the EA scar information **(see supplement, Case 3)**. In addition, pacing at longer cycle length (CL) than VT CL may also significantly influence the 12-lead ECG. In the study by Kuchar, a fixed pacing rate of 400ms was used, which may also partly explain the low predictive value of the algorithm to precisely localize the VT SoO.

In 2007, Segal et al.[6] correlated 12 lead ECG characteristics during VT with VT exit site determined by non-contact mapping. VT ECGs were categorized according to BBB configuration, frontal plane axis and R-wave transition. The VT exit site was defined as the point from which the rapidly expanding systolic activation on the isopotential

map occurred synchronous or just before (up to 40ms) QRS onset and was allocated to 9 predefined LV segments based on the 3D reconstruction of the endocardial LV surface using the Ensite system (Ensite 3000, Endocardial Solutions, Inc., St. Paul, MN, USA).

Figure 3.

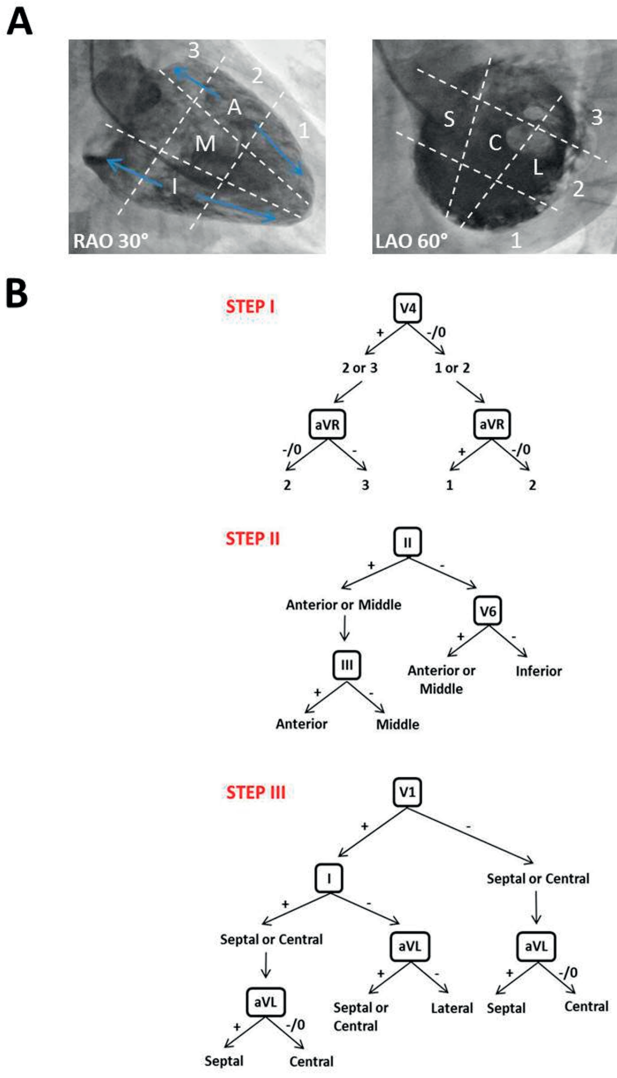

Algorithm proposed by Kuchar et al.[5] to predict the endocardial VT site of origin based on the 12-lead ECG VT morphology in patients with prior myocardial infarction. (Modified from Kuchar et al., J Am Coll Cardiol 1989)

Panel A: From two fluoroscopic projections (right anterior oblique [RAO] and left anterior oblique [LAO]) the LV endocardial surface is divided in 24 segments: 1, 2 and 3 indicate the apical, mid-ventricular and basal LV regions respectively; A, anterior; M, middle; I, inferior; S, septal; C, central and L, lateral.

Panel B: Proposed algorithm to identify the endocardial VT site of origin based on analysis of paced QRS in patients with myocardial infarction.

A total of 121 VTs from 51 patients with prior (single or multiple) MI were analyzed. All VT ECGs could be categorized in 10 ECG patterns, from which 8, accounting for 86 VTs (71%) had a PPV ≥70% for a predefined VT exit site region. Only the BBB morphology and the frontal plane axis were used in the construction of this algorithm since no consistent R-wave precordial transition pattern could be identified **(Table 1).** All LBBB VTs had a septal exit site and in contrast to Miller et al.'s, a PPV≥70% was more common for RBBB than for LBBB VTs (76% vs 43%). Rapid activation was often recorded from the mid LV regions which are less often involved in either anterior-apical or inferior-basal infarctions. VT exit sites were therefore likely to correspond with the true scar border zone.

Table 1. Algorithm proposed by Segal et al. to predict the endocardial VT site of origin according to a 9 LV regions model based on the 12-lead ECG VT morphology including BBB and frontal plane axis (Modified from Segal et al., J Cardiovasc Electrophysiol 2007)

	BBB	Axis	Exit	PPV%	Sensitivity%
1	RBBB	LS	Inferomedial/Inferobasal	100	100
2	RBBB	RS	Inferoapical	100	18
3	RBBB	RS	Inferoapical	77	59
4	RBBB	RI	Anteromedial	77	100
5	RBBB	LI	Anterobasal	100	100
6	LBBB	RS	Basoseptal	100	33
7	LBBB	LS	Medioseptal	100	35
8	LBBB	LS	Apicoseptal	22	100
9	LBBB	RI	Medioseptal	100	22

The application of distinct definitions for the VT SoO and the inclusion of different patient populations with different scar characteristics among studies (e.g. single prior MI in Miller's study, multiple prior MIs in Kuchar's and Segal's study) may also explain the inconsistent findings between algorithms.

More recently, the University of Michigan's group[7] demonstrated that the value of the 12-lead VT ECG for localizing the VT exit site improves substantially when using an automated computerized algorithm. To create the algorithm, digitalized 12-lead ECGs of pace-maps from the scar area of 34 patients with prior MI and the locations of the pace-maps based on a 10 LV regions model were used. Subsequently, the training data containing only pace-maps was validated by using the 12-lead ECGs of 58 VTs from 33 post-MI patients in which the VT exit site was determined by pace-mapping. The accuracy of the algorithm for assigning both the 12-lead ECG of pace-maps from the training sample and the VTs of the testing sample to the correct anatomic region was ≈ 70% (in comparison to an estimated accuracy of 19% for Miller's et al. and 36% for Segal's et al. algorithms) with a spatial resolution of 15 cm^2. The accuracy of the algorithm varied

from region to region and in contrast to Miller's et al. it was higher for anterior infarcts and worse for apical regions (≈50%)**(Table 2)**.

Table 2 summarizes the proposed algorithms to identify the endocardial VT SoO in patients with prior MI.

First author and year of publication	Number of patients	Number of analyzed VTs	Number of VTs in which the algorithm could be applied	Number of VTs correctly localized by algorithm	VT Site of Origin definition	Method	Based on
Miller 1988	102	182	87 (48%)	73 (84%)	Exit site/ Ablation target site	Activation mapping	11-region LV model by fluoroscopy
Kuchar 1989	42	44	44 (100%)	17 (39%)	Exit site	Pace-mapping	24-region LV model by fluoroscopy
Segal 2007	51	121	86 (71%)	8/9 (89%)	Exit site	Non-contact mapping	9-region LV model by ENSITE system
Yokokawa 2012	33	58	58 (100%)	41 (71%)	Exit site	Pace-mapping	10-region LV model by CARTO system

In all previously commented studies, the training cohort to create the algorithms differed from the validation cohort. This approach precludes correction for interindividual variations like LV and RV anatomy, rotation of the heart or lead placement[10], which may have also contributed to their limited accuracy to predict the VT SoO.

Site of origin as "target site for ablation"

Activation of the slow conducting critical isthmus does often not directly contribute to the 12-lead VT ECG. However, the combination of different 12-lead VT morphologies inducible in one patient may provide important, albeit indirect information for the location of an ablation target site. Wilber et al.[8] demonstrated that in patients with prior inferior MI inducible for two specific VT morphologies, one with LBBB and left superior axis and the other with RBBB and right superior axis, the critical isthmus site for both VTs can be located in the inferobasal LV, close to the mitral annulus. In this study, 4 out of 12 patients after inferior MI had these two inducible VT morphologies. In each of these 4 patients, participation of this "mitral isthmus" as critical slow conducting part of the reentrant circuit was demonstrated during both RBBB and LBBB tachycardias by entrainment mapping. A single RF application abolished both VT morphologies, suggesting that this critical site was shared by both VTs **(Figure 4).** Of interest, the BBB configuration and the frontal plane axis of the VTs were consistent among the 4 patients. However, some important differences in the precordial patterns were observed, sug-

gesting that in particular, the precordial leads are more influenced by interindividual variations such as shape of the heart and scar distribution **(Figure 5).** With increasing septal scar extension, also LBBB VTs with early precordial transition and inferior axis can be related to a mitral isthmus reentry circuit **(see Figure 5, Patient 4)**. In addition, with more apical scar extension, the precordial transition of RBBB VTs to a dominant negative QRS complex may be observed in V4 despite a basolateral exit site **(see Figure 5, Patients 1 and 3)**.

Figure 4.
Mitral isthmus related VT.

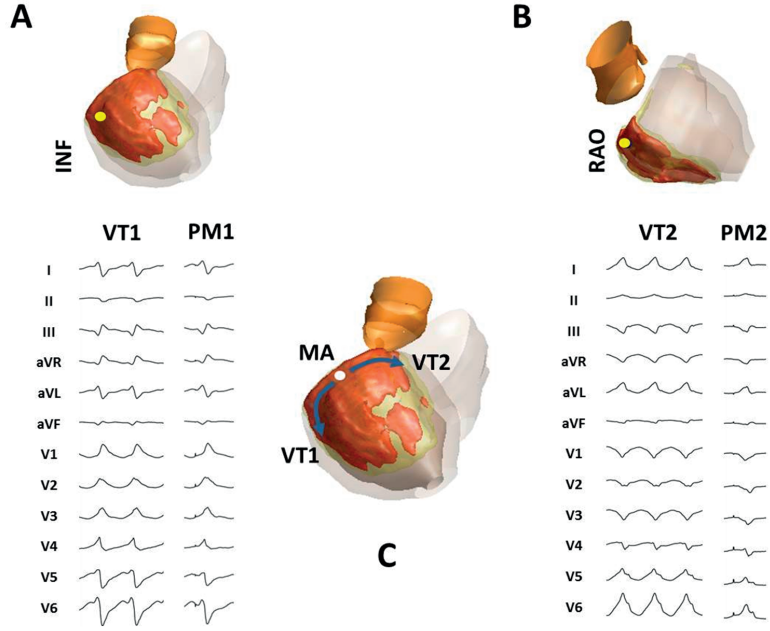

DE-MRI derived 3D reconstruction of the scar of a patient after inferior MI. Orange indicates core scar and yellow, border zone based on signal intensity (SI). Two VT morphologies were induced.
Panel A: VT1: RBBB morphology, RS axis. Panel B: VT2: LBBB morphology, LS axis. The best pace-map (indicated by a yellow dot) for VT1 was found in the basolateral aspect of the scar (PM1, panel A). The best pace-map for VT2 was found in the basoseptal aspect of the scar (PM2, panel B). The successful ablation site for both VTs, located in the basal LV close to the mitral annulus (MA) is indicated with a white dot. The blue arrows indicate the assumed direction of the activation wavefront during VT1 and VT2, respectively.

Figure 5.

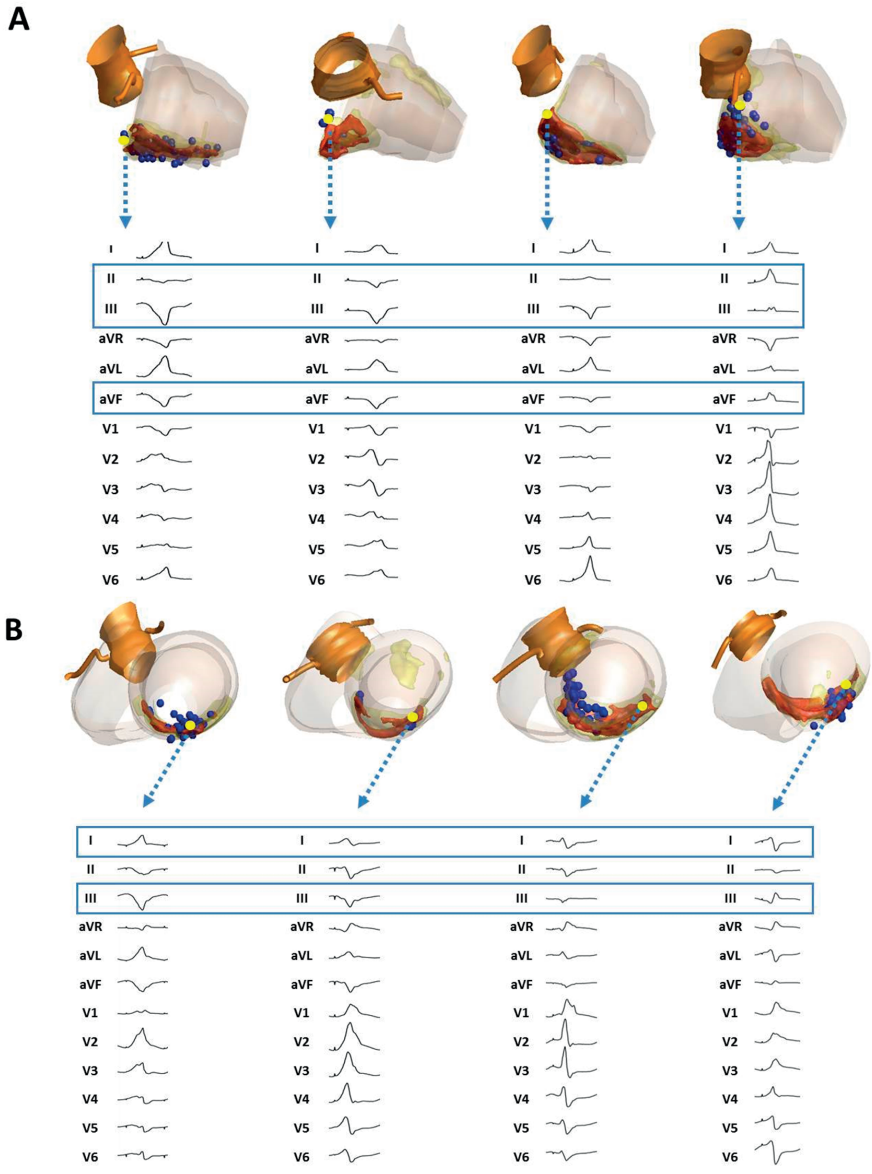

DE-MRI derived 3D reconstructions of scars of 4 patients with prior inferior MI are shown. Orange indicates core scar and yellow, border zone based on SI. The pacing site that corresponds to the displayed QRS paced morphologies are marked by yellow dots.

Panel A: paced 12-lead ECGs at the septal border of the inferior scar. All paced QRS had a LBBB morphology and monophasic R waves in I, V5 and V6. With higher septal scar extension, the frontal plane axis shifts gradually from left superior to left inferior axis.

Panel B: paced 12-lead ECGs at the lateral border of the inferior scar. All paced QRS had a RBBB morphology and a terminal S wave in V5 and V6. With higher lateral scar extension, the morphology of I changes from a monophasic R wave to a progressively pronounced terminal S wave and the morphology of III from a QS to a progressively higher amplitude of the terminal R wave.

VALUE OF THE 12-LEAD ECG TO PREDICT AN EPICARDIAL VERSUS AN ENDOCARDIAL LEFT VENTRICULAR VT SITE OF ORIGIN

Prior reports

Critical parts of the reentrant circuit that are located deep in the myocardium or at the subepicardium can often not be abolished by endocardial ablation. This is more common in patients with nonischemic cardiomyopathy (NICM), in which the VT substrate is frequently located intramurally or subepicardially, often requiring an epicardial or a combined endo-epicardial ablation to achieve procedural success[11-12].

DE-MRI performed prior to mapping and ablation can delineate the 3D scar geometry and its relationship to the endocardial and epicardial surfaces. Based on the MRI derived scar information, patients who may benefit from an endocardial, epicardial or combined approach can be selected[13]. However, currently MRI imaging in patients with implanted defibrillators is only available at selected centres. In addition, artifacts due to leads and pulse generators may hamper detailed analysis of, in particular, anterior basal segments[14]. EA voltage mapping may be an alternative to detect myocardial scar. However, endocardial bipolar voltage mapping is limited by the presence of endocardial viable myocardium in patients with mid-myocardial or subepicardial scars[15]. The value of endocardial unipolar voltage mapping to unmask epicardial scars has been recently suggested[16]. However, if compared with DE-MRI, unipolar endocardial voltage mapping has only a moderate sensitivity and specificity for detecting subepicardial scars[17].

Using the 12-lead ECG of the VT to determine the required access is appealing. Berruezo et al.[18] were the first proposing ECG criteria to distinguish an epicardial from an endocardial LV-VT SoO in a mixed group of patients with ischemic and NICM. All criteria are based on the assumption that ventricular activation originating from the epicardium is followed by a transmural activation delay until the subendocardial Purkinje system is reached. This propagation pattern will prolong the initial part of the QRS resulting in visible slurring and/or widening.

LBBB VTs were excluded from the initial analysis as these VTs were considered to originate from the interventricular septum.

A Pseudodelta wave (PDW) ≥ 34ms: interval from the earliest ventricular activation to the earliest rapid deflection in any precordial lead; an *Intrinsicoid deflection time (IDT) ≥ 85ms*: interval from the earliest ventricular activation to the peak of the R wave in V2 and a *shortest RS complex (SRS) ≥ 121ms*: interval from the earliest ventricular activation to the nadir of the first S wave in any precordial lead, predicted the failure of an

endocardial VT ablation with a high sensitivity and specificity in patients with SHD **(see supplement, Case 6).**

Following the same concept, Daniels et al.[19] could show that a *maximum deflection index (MDI) ≥55ms***,** defined as the interval from the earliest ventricular activation to the peak of the largest amplitude deflection in each precordial lead (taking the lead with the shortest time) divided by the QRS duration, identified an epicardial VT origin with a high sensitivity and specificity (>95%) in patients with idiopathic VTs with both RBBB and LBBB morphology **(Figure 6).**

Figure 6.

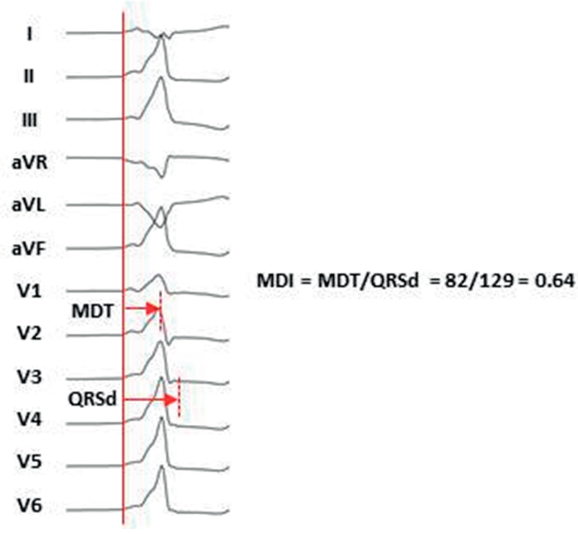

Determination of the MDI: the interval between the earliest ventricular activation and the maximum deflection in each precordial lead (taking the shortest interval) is divided by the QRS duration. A MDI ≥55ms had a high sensitivity and specificity to identify an epicardial VT origin in patients without structural heart disease. (Modified from Daniels et al., Circulation 2006)

Bazan et al.[20] reported that these previously suggested *interval criteria,* although useful to identify an epicardial LV-VT site of origin, did not perform uniformly for all LV regions. Additional site-specific *morphological criteria* were proposed based on the concept that the initial vector of impulse propagation from the epicardium towards the endocardium would result in the presence of an initial Q wave in the ECG leads reflecting the site of epicardial activation (or the absence of a Q wave in opposite leads). A Q wave in lead I for basal superior and apical superior VTs was associated with an epicardial site of origin. In addition, the absence of Q waves in any inferior leads for basal superior VT or a Q wave in inferior leads with VTs arising from the basal inferior and apical inferior LV also indicated an epicardial SoO.

Since the substrate for VTs in patients with NICM is often located in the basal LV, clustering around the mitral and aortic annulus, Vallès et al.[21], from the same group, evaluated the value of the previously proposed interval and morphological criteria to predict an epicardial VT origin from this specific LV region. Out of 24 VTs with RBBB morphology originated in the basal superior or lateral LV from 14 patients with NICM, 16 had an epicardial origin on the basis of entrainment and/or pace-mapping. Applying the interval ECG criteria, only a significantly longer duration of the QRS and a longer shortest RS complex were observed for epicardial compared to endocardial VTs. Of note, the presence of a Q wave in lead I had the highest individual sensitivity and specificity (88%) of all tested criteria. However, since a single criterion had a limited predictive value, a 4-step algorithm that included interval and morphological criteria was proposed reaching a high sensitivity and specificity for identifying an epicardial VT SoO from the basal or lateral LV in the preselected group of patients with NICM **(Figure 7).**

Recently, Yokokawa et al.[22] demonstrated that the accuracy of the 12-lead ECG for differentiating between endocardial and epicardial pace-map sites improved when applying a computerized algorithm compared to prior reported algorithms.

Figure 7.

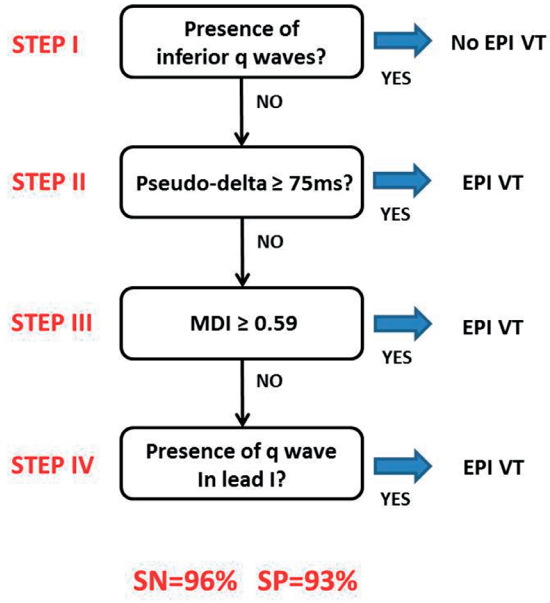

Multistep algorithm to identify an epicardial left ventricular VT site of origin from the basal superior and lateral LV in patients with NICM. The cut-off values of the PDW and MDI were modified to increase its individual predictive value. (Modified from Vallès et al. Cir Arrhythm Electrophysiol 2010)

Limitations of the 12-lead ECG to predict an epicardial VT site of origin

The ECG criteria for identifying an epicardial LV VT SoO were derived from the analysis of pace-maps and a limited number of VTs from a population mainly comprised of patients without SHD or with NICM **(Table 3)**. Martinek et al.[23] showed that in post-MI patients, both the interval and the morphological ECG criteria failed to distinguish an epicardial from an endocardial LV VT SoO defined as the *successful ablation site*. Two factors may explain this finding. The presence of typical Q waves in the VT ECGs of patients with prior MI precludes the use of morphological ECG criteria and, when present in the precordial leads, Q waves may interfere with the measurement of all interval criteria **(see supplement, Case 6).** Perhaps even more importantly, the VT 12-lead ECG provides information about the VT exit site from the scar border, but successful ablation is often performed at other critical parts of the reentrant circuit. In particular, in patients with prior MI, both the presence of wall thinning and the subendocardial location of parts of the reentry circuit may allow successful ablation of VTs with an epicardial exit site from the endocardium. Accordingly, the number of VTs with an epicardial exit site may be underestimated.

Piers et al.[24] could recently demonstrate that when applied to clinically documented VTs (conventionally recorded with 25mm/s, 10mm/mV and measured with manual calipers) from patients with NICM, neither interval nor morphological ECG criteria could differentiate between an endocardial and an epicardial VT SoO defined as successful ablation site. For induced VTs (recorded on an electrophysiological recording system and measured with electronic calipers at 100mm/s), the interval criteria could distinguish between an endocardial and epicardial VT SoO for slow VTs but could also not reliably identify an epicardial VT origin in patients with fast VTs (CL≤350ms) or in patients off amiodarone. The absence of a clear isoelectric interval and/or the overlap of the QRS complex with the previous T wave during fast VTs may hamper an accurate identification of the QRS onset, which is mandatory for the measurement of all interval criteria. However, for induced VTs, the morphological criteria appeared to be not affected by the VT CL or amiodarone use. The latter confirms the findings from Vallès et al., who, as previously stated, has demonstrated that the presence of a Q wave in lead I had the highest individual accuracy for identifying an epicardial VT origin in patients with NICM **(Figure 8)**.

There are limited data on the value of the 12-lead VT ECG to predict an epicardial VT origin from the RV. Bazan et al.[25] analyzed 180 endocardial and 134 epicardial pace-maps from a group of 13 patients without structural heart disease (7/13) and RV cardiomyopathy (8/13). No interval criterion was able to distinguish an epicardial from an endocardial RV pace-map site in this population. Again, site-specific morphological criteria seemed to be useful for identifying an epicardial RV pace-map site. However, this finding was based on only 5 successfully ablated VTs from the epicardial RV.

Table 3. Proposed criteria to identify an epicardial left ventricular VT site of origin

First author and year of publication	Population	Number of patients	Number of paced-maps/ VTs analyzed	Criteria	Sensitivity	Specificity
Berruezo 2004	Post-MI/ NICM	67	Not provided/69	Pseudodelta wave ≥ 34ms Intrinsicoid deflexion time ≥ 85ms Shortest RS interval ≥ 121ms	83% 87% 76%	95% 90% 85%
Daniels 2006	Idiopathic	12	0/12	Maximum deflexion index ≥ 0.55	100%	99%
Bazan 2007	Idiopathic/ NICM	28	636/19	Q wave in I: Basal superior LV Apical superior LV Q wave in inferior leads: Basal inferior LV Apical inferior LV	 86% 84% 74% 94%	 81% 78% 51% 61%

VALUE OF THE 12-LEAD ECG TO PREDICT THE UNDERLYING SUBSTRATE FOR VT

In patients with NICM, the VT 12-lead ECG morphology helps to predict the location and extension of the arrhythmogenic substrate, which may have implications for selecting the primary ablation approach (endocardial vs endo/epicardial) and for estimating the probability of procedural success and patient prognosis.

Piers et al.[17] demonstrated that 17 of 19 patients (89%) with NICM referred for VT ablation with DE-MRI integration had one of two typical scar patterns (basal anteroseptal or inferolateral). All but one patient had at least 1 of 3 characteristic VT ECG morphologies, diagnostic for one of these two typical scar locations. All patients with RBBB morphology, positive precordial concordance and inferior axis VTs or LBBB morphology, early precordial transition (≤V3) and inferior axis VTs had an anteroseptal scar whereas all patients with RBBB morphology, late precordial transition and right (superior or inferior) axis VTs had an inferolateral scar **(Figure 9)**. The majority of ablation target sites for patients with anteroseptal scars were located in the aortic root or in the basal anteroseptal LV endocardium **(see supplement, Case 7).** In these patients, if ablation via the coronary sinus and its branches fails, epicardial mapping and ablation using a conventional subxiphoid approach is unlikely to be appropriate due to the presence of the overlying left atrial appendage, coronary arteries and/or epicardial fat at the epicardial LV summit. On the contrary, in patients with inferolateral scars, the majority of ablation target sites could be reached from the LV epicardium. Epicardial mapping was not hampered by overlying structures like the left atrial appendage, a thick fat layer

Figure 8.

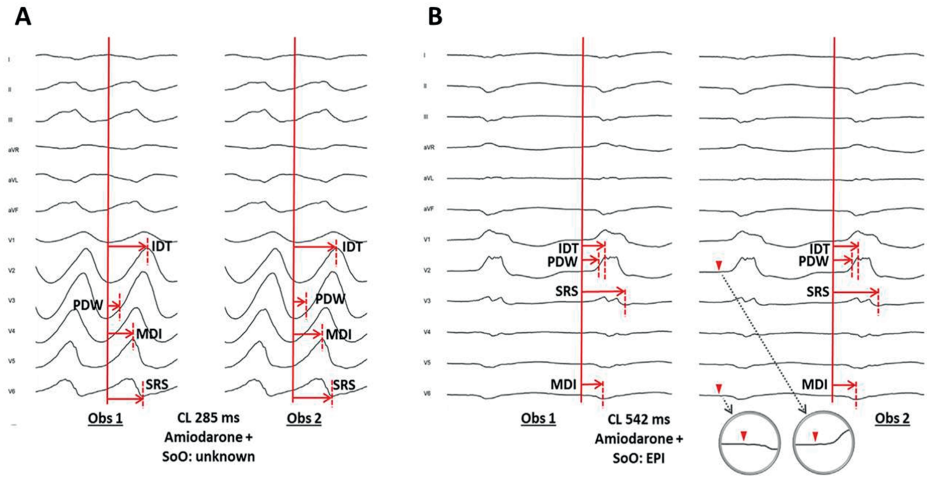

Reported interval and morphological ECG criteria for identifying a LV epicardial VT site of origin are assessed by two different observers for a fast (panel A) and a slow (panel B) VT. Of note, for the fast VT the QRS onset is defined differently, affecting the measurement of all the interval criteria. (Modified from Piers et al., Heart Rhythm 2014)

or coronary arteries in these patients; however RF delivery may need to be withheld if damage of the coronary arteries or the phrenic nerve cannot be excluded. Oloriz et al.[26] confirmed subsequently these findings in a larger cohort of patients.

As previously indicated, the VT substrate in patient with NICM is often located in the basal LV, around the valvular annuli with variable extension towards the LV apex. Out of 76 patients with NICM referred for VT ablation, Frankel et al.[27] identified 32 (42%) who had spontaneous or induced VTs with a morphology suggestive of an apical exit site. An *apical VT morphology* was defined as a VT with LBBB morphology and late precordial transition (≥V5) to a dominant positive QRS complex or with RBBB morphology and early precordial transition (≤V3) to a dominant negative QRS complex. Markedly, patients with apical VT morphologies had larger scar areas delineated by voltage mapping and a worse prognosis, with a higher likelihood of requiring heart transplant or left ventricular assist devices because of advanced heart failure.

Finally, data on the value of the 12-lead ECG for predicting the underlying substrate for VTs arising from the RV are scarce. Hoffmayer et al.[28] compared the 12-lead ECG morphology of VTs with LBBB and inferior axis from 42 patients with idiopathic RVOT VT and 16 with arrhythmogenic right ventricular cardiomyopathy (ARVC). Duration of the QRS in lead I ≥120ms, earliest onset of QRS in lead V1, presence of QRS notching in at least one lead and a precordial transition at V_5 or later were independent predictors of ARVC. Using these ECG features during VT and the presence/absence of negative T waves in

leads V1-V3 during sinus rhythm, the same authors constructed a risk score for ARVC[29]. A score ≥5 (maximum score 8 points) identified ARVC as underlying substrate for VT with a PPV of 100% and a negative PV of 91%.

Figure 9.

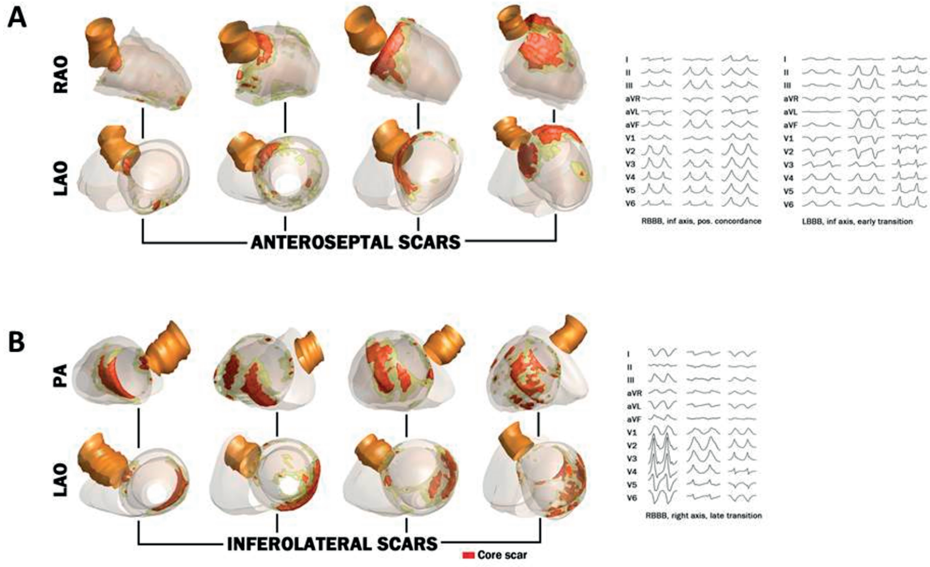

Typical scar patterns and associated 12-lead VT ECGs in non-ischemic cardiomyopathy (Modified from Piers et al., Circ Arrhythm Electrophysiol 2013)
DE-MRI derived 3D reconstructions of scars from patients with NICM are shown. Orange indicates core scar and yellow, border zone. Panel A: examples of typical basal anteroseptal scars and related 12-lead VT ECGs. Panel B: examples of typical inferolateral scars and related 12-lead VT ECGs.

SUMMARY

Several algorithms for identifying the *VT origin* based on the analysis of the 12-lead VT ECG have been suggested. These algorithms have applied different definitions for *VT site of origin* that include VT exit sites but also reentry circuit exit sites and isthmus sites. In addition, they have been validated by different mapping techniques encompassing activation and entrainment mapping, but also pace-mapping. None of the algorithms integrated information on the scar extension and distribution, which may increase the accuracy of the ECG to precisely predict the VT origin. A systematic re-evaluation of the value of the 12-lead ECG for VT ablation in the context of 3D EAM, scar imaging and changing ablation strategies with a shift from targeting clinical and induced VTs to substrate ablation approaches is needed.

REFERENCES

1. Stevenson WG, Wilber DJ, Natale A, Jackman WM, Marchlinski FE, Talbert T, Gonzalez MD, Worley SJ, Daoud EG, Hwang C, Schuger C, Bump TE, Jazayeri M, Tomassoni GF, Kopelman HA, Soejima K, Nakagawa H; Multicenter Thermocool VT Ablation Trial Investigators. Irrigated catheter ablation guided by electroanatomic mapping for recurrent ventricular tachycardia after myocardial infarction: the multicenter thermocool ventricular tachycardia ablation trial. *Circulation*. 2008;118:2773–2782.
2. Piers SR, Leong DP, van Huls van Taxis CF, Tayyebi M, Trines SA, Pijnappels DA, Delgado V, Schalij MJ, Zeppenfeld K. Outcome of ventricular tachycardia ablation in patients with nonischemic cardiomyopathy: the impact of noninducibility. *Circ Arrhythm Electrophysiol*. 2013;6:513-521.
3. Park KM, Kim YH, Marchlinski FE. Using the surface electrocardiogram to localize the origin of idiopathic ventricular tachycardia. *PACE*. 2012;35:1516-1527.
4. Miller JM, Marchlinski FE, Buxton AE, Josephson ME. Relationship between the 12-lead electrocardiogram during ventricular tachycardia and endocardial site of origin in patients with coronary artery disease. *Circulation*. 1988;77:759-766.
5. Kuchar DL, Ruskin JN, Garan H. Electrocardiographic localization of the site of origin of ventricular tachycardia in patients with prior myocardial infarction. *J Am Coll Cardiol*. 1989;13:893-900.
6. Segal OR, Chow AWC, Wong T, Trevisi N, Lowe MD, Davies DW, Della Bella P, Packer DL, Peters NS. A novel algorithm for determining endocardial VT exit site from 12-lead surface ECG characteristics in human, infarct-related ventricular tachycardia. *J Cardiovasc Electrophysiol*. 2007;18:161-168.
7. Yokokawa M, Liu TY, Yoshida K, Scott C, Hero A, Good E, Morady F, Bogun F. Automated analysis of the 12-lead electrocardiogram to identify the exit site of postinfarction ventricular tachycardia. *Heart Rhythm*. 2012;9:330-334.
8. Wilber DJ, Kopp DE, Glascock DN, Kinder CA, Kall JG. Catheter ablation of the mitral isthmus for ventricular tachycardia associated with inferior infarction. *Circulation*. 1995;92:3481-3489.
9. De Chillou C, Groben L, Magnin-Poull I, Andronache M, Magdi Abbas MM, Zhang N, Abdelaal A, Ammar S, Sellal JM, Schwartz J, Brembilla-Perrot B, Aliot E, Marchlinski FE. Localizing the critical isthmus of postinfarct ventricular tachycardia: The value of pace-mapping during sinus rhythm. *Heart Rhythm*. 2014;11:175-181.
10. Anter E, Frankel DS, Marchlinski FE, Dixit S. Effect of electrocardiographic lead placement on localization of outflow tract tachycardias. *Heart Rhythm*. 2012;9:697-703.
11. Hsia HH, Callans DJ, Marchlinski FE. Characterization of endocardial electrophysiological substrate in patients with nonischemic cardiomyopathy and monomorphic ventricular tachycardia. *Circulation*. 2003;108:704-710.
12. Soejima K, Stevenson WG, Sapp JL, Selwyn AP, Couper G, Epstein LM. Endocardial and epicardial radiofrequency ablation of ventricular tachycardia associated with dilated cardiomyopathy. The importance of low-voltage scars. *J Am Coll Cardiol*. 2004;43:1834-42.
13. Andreu D, Ortiz-Pérez JT, Boussy T, Fernández-Armenta J, de Caralt TM, Prat-González S, Mont L, Brugada J, Berruezo A. Usefulness of contrast-enhanced cardiac magnetic resonance in identifying the ventricular arrhythmia substrate and the approach needed for ablation. *Eur Heart J*. 2014;35:1316-1326.
14. Dickfeld R, Tian J, Ahmad G, Jimenez A, Turgeman A, Kuk R, Peters M, Saliaris A, Saba M, Shorofsky S, Jeudy J. MRI-Guided ventricular tachycardia ablation: integration of late gadolinium-enhanced 3D scar in patients with implantable cardioverter-defibrillators. *Circ Arrhythm Electrophysiol*. 2011;4:172-184.

15. Piers SR, van Huls van Taxis CF, Tao Q, van der Geest RJ, Askar SF, Siebelink HM, Schalij MJ, Zeppenfeld K. Epicardial substrate mapping for ventricular tachycardia ablation in patients with non-ischemic cardiomyopathy: a new algorithm to differentiate between scar and viable myocardium developed by simultaneous integration of computed tomography and contrast-enhanced magnetic resonance imaging. *Eur Heart J*. 2013;34:586-596.
16. Hutchinson MD, Gerstenfeld EP, Desjardins B, Bala R, Riley MP, Garcia FC, Dixit S, Lin D, Tzou WS, Cooper JM, Verdino RJ, Callans DJ, Marchlinski FE. Endocardial unipolar voltage mapping to detect epicardial ventricular tachycardia substrate in patients with nonischemic left ventricular cardiomyopathy. *Circ Arrhythm Electrophysiol*. 2011;4:49-55.
17. Piers SRD, Tao Q, van Huls van Taxis CFB, Schalij MJ, van der Geest RJ, Zeppenfeld K. Contrast-enhanced MRI-derived scar patterns and associated ventricular tachycardias in nonischemic cardiomyopathy. Implications for ablation strategy. *Circ Arrhythm Electrophysiol*. 2013;6:875-883.
18. Berruezo A, Mont L, Nava S, Chueca E, Bartholomay E, Brugada J. Electrocardiographic recognition of the epicardial origin of ventricular tachycardia. *Circulation*. 2004; 109:1842-1847.
19. Daniels DV, Lu YY, Morton JB, Santucci PA, Akar JG, Green A, Wilber DJ. Idiopathic epicardial left ventricular tachycardia originating remote from the sinus of Valsalva. Electrophysiological characteristics, catheter ablation, and identification from the 12-lead electrocardiogram. *Circulation*. 2006;113:1659-1666.
20. Bazan V, Gerstenfeld EP, Garcia FC, Bala R, Rivas N, Dixit S, Zado E, Callans DJ, Marchlinski FE. Site-specific twelve-lead ECG features to identify an epicardial origin for left ventricular tachycardia in the absence of myocardial infarction. *Heart Rhythm*. 2007; 4:1403-1410.
21. Vallès E, Bazan V, Marchlinski FE. ECG criteria to identify epicardial ventricular tachycardia in nonischemic cardiomyopathy. *Circ Arrhythm Electrophysiol*. 2010;3:63-71.
22. Yokokawa M, Yon Jung D, Joseph KK, Hero AO, Morady F, Bogun F. Computerized analysis of the 12-lead electrocardiogram to identify epicardial ventricular tachycardia exit sites. *Heart Rhythm*. 2014;11:1966-1973.
23. Martinek M, Stevenson WG, Inada K, Tokuda M, Tedrow UB. QRS characteristics fail to reliably identify ventricular tachycardias that require epicardial ablation in ischemic heart disease. *J Cardiovasc Electrophysiol*. 2012;23:188-193.
24. Piers SRD, de Riva Silva M, Kapel GFL, Trines SA, Schalij MJ, Zeppenfeld K. Endocardial or epicardial ventricular tachycardia in nonischemic cardiomyopathy?. The role of 12-lead ECG criteria in clinical practice. *Heart Rhythm*. 2014;11:1031-1039.
25. Bazan V, Bala R, Garcia FC, Sussman JS, Gerstenfeld EP, Dixit S, Callans DJ, Zado E, Marchlinski FE. Twelve-lead ECG features to identify ventricular tachycardia arising from the epicardial right ventricle. *Heart Rhythm*. 2006;3:1132-1139.
26. Oloriz T, Silberbauer J, Maccabelli G, Mizuno H, Baratto F, Kirubakaran S, Vergara P, Bisceglia C, Santagostino G, Marzi A, Sora N, Roque C, Guarracini F, Tsiachris D, Radinovic A, Cireddu M, Sala S, Gulletta S, Paglino G, Mazzone P, Trevisi N, Della Bella P. Catheter ablation of ventricular arrhythmia in nonischemic cardiomyopathy. Anterseptal versus inferolateral scar sub-types. *Circ Arrhythm Electrophysiol*. 2014;7:414-423.
27. Frankel DS, Tschabrunn CM, Cooper JM, Dixit S, Gerstenfeld EP, Riley MP, Callans DJ, Marchlinski FE. Apical ventricular tachycardia morphology in left ventricular nonischemic cardiomyopathy predicts poor transplant-free survival. *Heart Rhythm*. 2013;10:621-626.
28. Hoffmayer KS, Machado ON, Marcus GM, Yang Y, Johnson CJ, Ermakov S, Vittinghoff E, Pandurangi U, Calkins H, Cannom D, Gear KC, Tichnell C, Park Y, Zareba W, Marcus FI, Scheinman MM. Electrocardiographic comparison of ventricular arrhythmias in patients with arrhythmogenic right

ventricular cardiomyopathy and right ventricular outflow tract tachycardia. *J Am Coll Cardiol*. 2011;58:831-838.

29. Hoffmayer KS, Bhave PD, Marcus GM, James CA, Tichnell C, Chopra N, Moxey L, Krahn AD, Dixit S, Stevenson W, Calkins H, Badhwar N, Gerstenfeld EP, Scheinmann MM. An electrocardiographic scoring system for distinguishing right ventricular outflow tract arrhythmias in patients with arrhythmogenic right ventricular cardiomyopathy from idiopathic ventricular tachycardia. *Heart Rhythm*. 2013;10:477-482.

SUPPLEMENTARY CASE 1

72 years male, 12 years after large anterior MI, clinical VTCL 548ms

Panel A: The clinical VT (VT1) had RBBB morphology with early precordial transition (V2) and right superior axis. The RV apex (RVa) catheter served as a reference during VT activation mapping. RVa activation is indicated by a continuous blue line. On the ECG, the QRS onset is difficult to determine. Two potential onsets (102 and 180ms before RVa) are indicated with dashed blue lines. Electroanatomical (EA) endocardial bipolar voltage map of the LV in RAO, LAO and inferior views shows a large low voltage area in the anterior wall extending to the septum and lateral wall (voltages are color coded according to the bar).

Panel B: Activation map during VT1 (AP and inferior views) displayed as isochronal map. Black tags indicate LV sites activated 180ms before the RVa, which are located within the scar based on voltage mapping. Blue tags indicate LV sites activated 102ms before the RVa, which coincides with the most obvious QRS onset, and are located in normal voltage areas. These sites were considered as the probable VT exit site. However, entrainment mapping at these locations showed fusion and a post pacing interval (PPI) exceeding VTCL>70ms. During detailed endocardial mapping, no mid-diastolic activity or isthmus sites based on entrainment mapping could be identified. After endocardial ablation failure, an epicardial ablation approach was scheduled.

At the beginning of the second procedure, a different slow VT (VT2, panel C) with LBBB morphology, V4 transition and left inferior axis was induced. The RVa timing is indicated by a continuous blue line. The QRS onset is indicated by a dashed blue line. The best endocardial pace-map site for VT2 at the basoseptal border of the scar is indicated by a yellow tag (panel D, top). During activation mapping (panel D, bottom) activation of this site coincided with the QRS onset (indicated by a blue tag). However, entrainment mapping resulted in fusion with a PPI exceeding VTCL>70ms. Limited epicardial activation mapping was performed during VT2 (mapped area indicated by the dashed white line) (panel E). The direction of the activation wave front is indicated by a white arrow. The reentry circuit entrance site confirmed by entrainment mapping (indicated by a green dot) was found in the apicoseptal epicardial LV. Please note the very long electrogram-to-QRS onset interval at this site. With the first RF application at this position, VT2 slowed. The VT isthmus site (indicated by a white dot and confirmed by entrainment) was localized slightly superior. With a second RF application, VT terminated. The presumed reentry exit site is indicated by a yellow dot. Please note the long distance to the exit site from the scar, where the best endocardial pace-map was obtained.

The VT morphology is mainly dependent on the site(s) where the wavefront emerges from the scar border to activate the normal myocardium. If the reentry exit site and the exit site from the scar do not correspond, the accuracy of the 12-lead ECG to predict the VT origin is limited and may direct to wrong target areas.

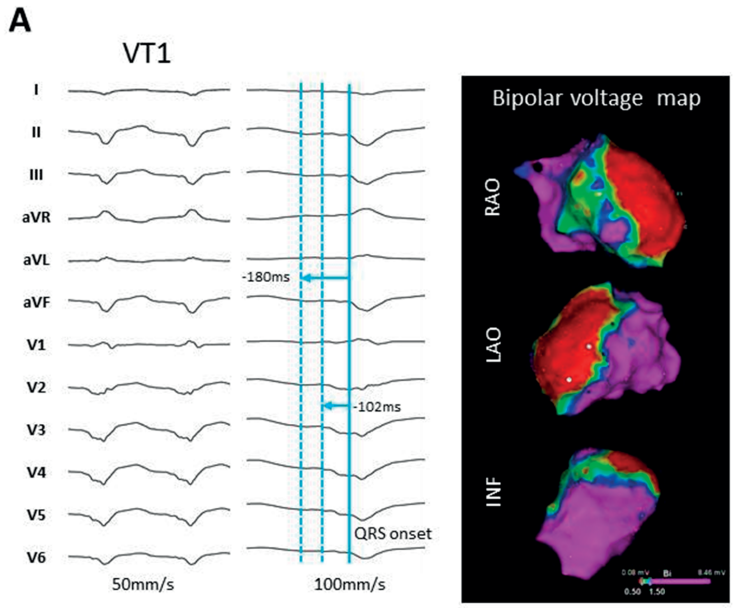
A
VT1
I
II
III
aVR
aVL
aVF
V1
V2
V3
V4
V5
V6
-180ms
-102ms
QRS onset
50mm/s
100mm/s
Bipolar voltage map
RAO
LAO
INF

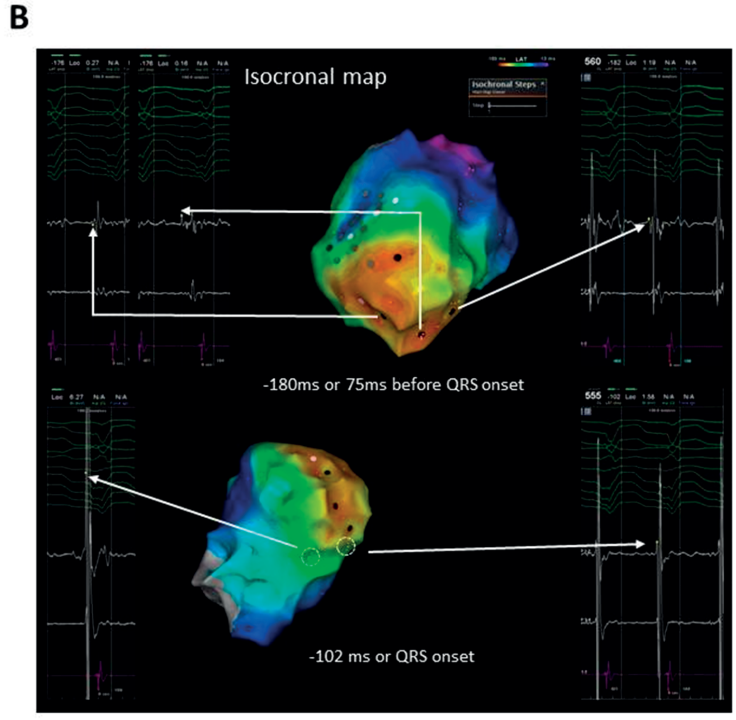
B
Isocronal map
-180ms or 75ms before QRS onset
-102 ms or QRS onset

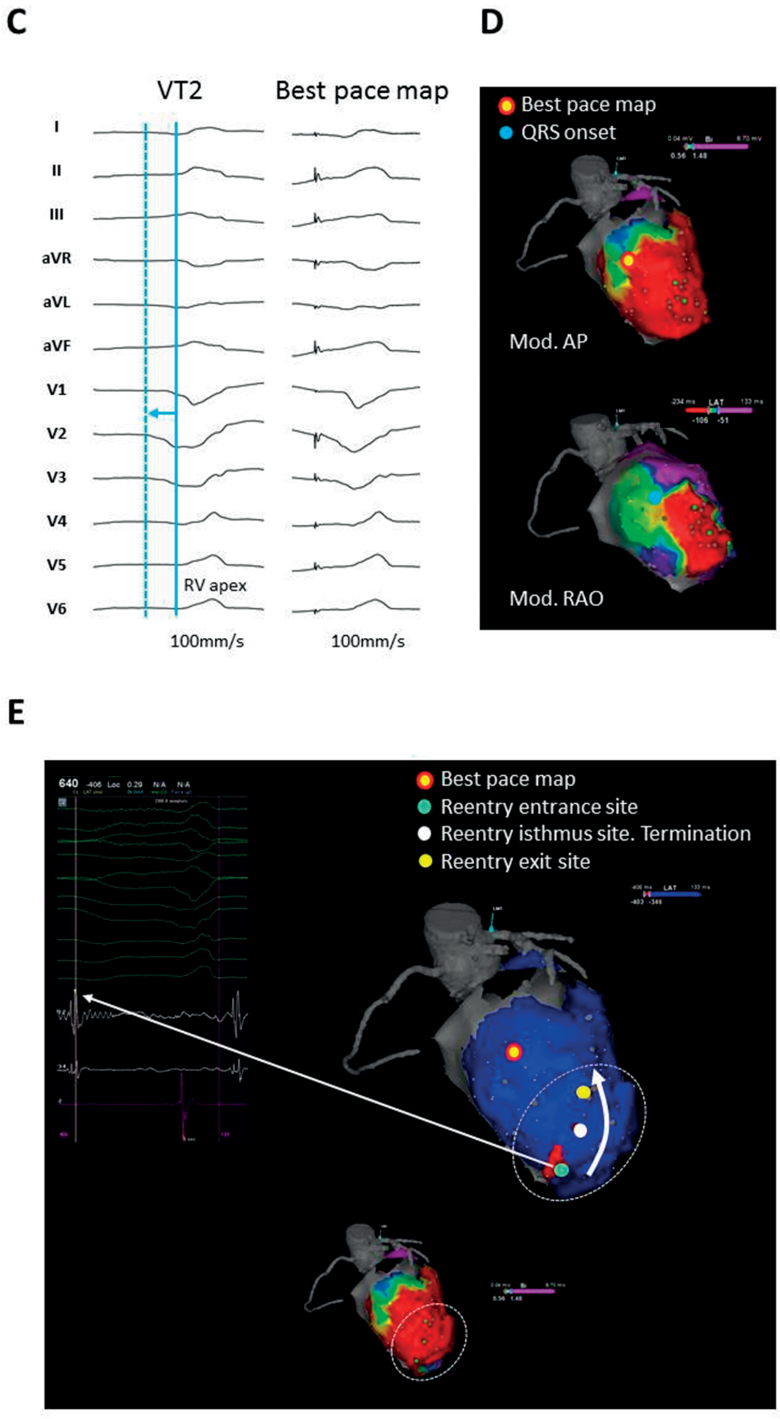
C
VT2
Best pace map
I
II
III
aVR
aVL
aVF
V1
V2
V3
V4
V5
V6
RV apex
100mm/s
100mm/s
D
Best pace map
QRS onset
Mod. AP
Mod. RAO
E
Best pace map
Reentry entrance site
Reentry isthmus site. Termination
Reentry exit site

SUPPLEMENTARY CASE 2

52 years male, 9 years after anterior MI, clinical VTCL 352ms

Panel A. Electroanatomical (EA) endocardial bipolar voltage map of the LV in a modified RAO view (left), and of the LV and RV in a modified superior view (right). Voltages are color coded according to the bar. Yellow tags indicate pacing sites around the EA scar; the numbers correspond to the numbers of the paced 12 lead ECG morphologies (Panel E). Best pace-map site and site of VT termination are indicated. Panel B: LV angiogram during diastole and systole showing a small apical aneurysm corresponding with the dense apical scar on EAM. Panel C: fluoroscopic views of the LV in RAO and LAO. Note the calcification of the aneurysm (white arrows). The position of the ablation catheter (red arrows) corresponds to the green tag, panel A.

The clinical VT (Panel D) had LBBB morphology with late transition and left superior axis and a predicted apicoseptal SoO/exit site according to Miller[4], Kuchar[5] and Segal[6].

However, pacing from the LV could not reproduce the VT morphology. The best pace-map was recorded during pacing at the RV septum (panel A,E). Limited entrainment mapping (not shown) could confirm the apical LV as outer loop and the RV apical septum as reentry circuit exit site (RF at this site abolished VT) which coincided with the RV scar border zone. The VT reentry circuit involved the septum and perhaps the subepicardial LV. Please note the changes of the paced QRS from left superior to right superior axis with only little changes in the precordial lead transition if pacing sites move from septal to anterolateral. These small changes may be explained by the limited lateral and anterior scar extension.

In addition to prior algorithms it is important to consider the RV as VT SoO.

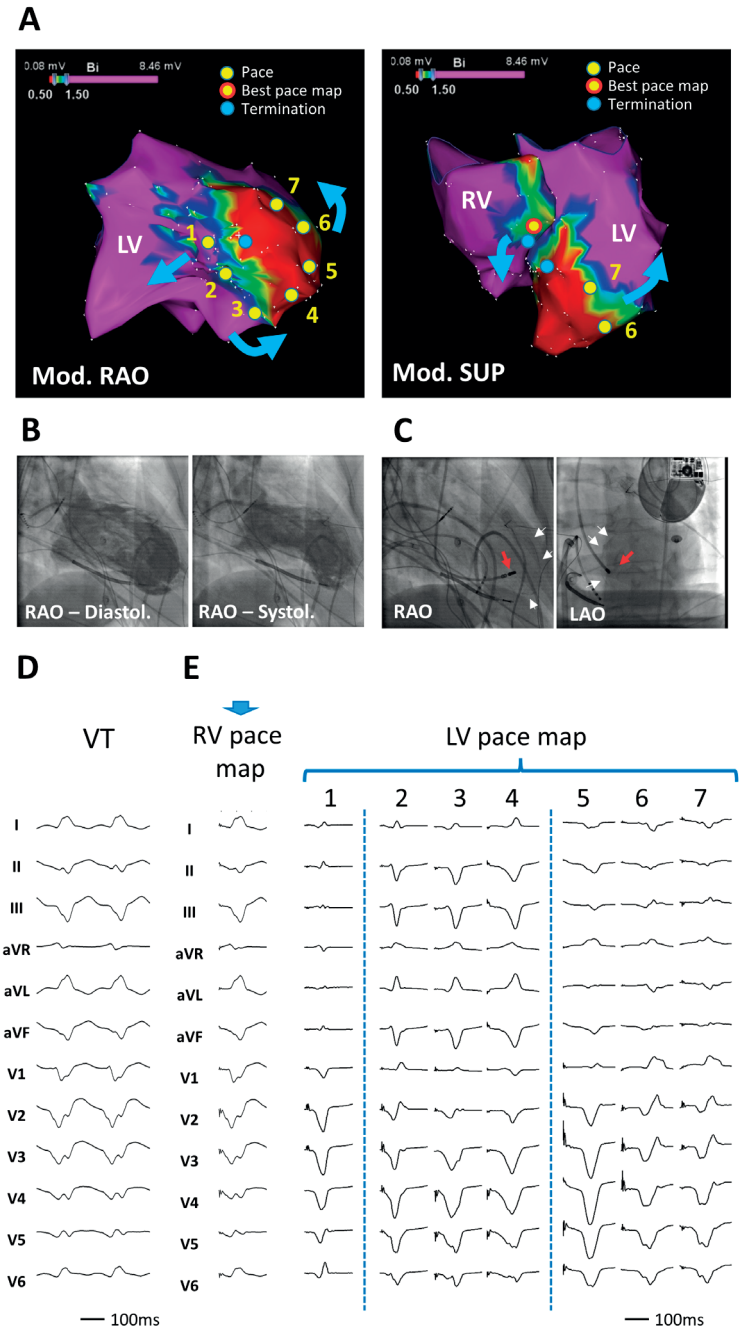
A
0.08 mV
Bi
8.46 mV
0.50 1.50
Pace
Best pace map
Termination
LV
RV
Mod. RAO
Mod. SUP
B
RAO – Diastol.
RAO – Systol.
C
RAO
LAO
D
VT
E
RV pace map
LV pace map
1 2 3 4 5 6 7
I
II
III
aVR
aVL
aVF
V1
V2
V3
V4
V5
V6
100ms
100ms

SUPPLEMENTARY CASE 3

65 years male, 5 years after small inferior MI, clinical VTCL 320ms

Panel A. EA endocardial bipolar voltage map of the LV in a modified posterior view (PA) rotated to the bottom (left) and standard PA (right) view (color coding according to the bar). Tags represent catheter positions as indicated; numbers correspond to the numbers of the paced 12 lead ECG morphologies (Panel C).

The clinical VT (panel B) had RBBB morphology with late transition (V6) and left superior axis and a predicted inferobasal SoO by Miller[4] and Segal[6]. Despite the small EA scar the paced QRS morphology changed from LBBB with early transition (V2) and left superior axis at pacing site 2 (inferoseptal) to RBBB with transition at V3 and left superior axis at site 3 (basal inferior) and to RBBB with late transition (V5) and left superior axis at site 5. Site 5 was the best albeit not perfect pace-map site. During pacing within this small area, the propagation direction changed from septal, to apical to lateral (indicated by the blue arrows). Based on the careful analysis of the paced-ECG the assumed activation during VT occurred in an apical to basal direction followed by two wave fronts in a septal (towards 2) and lateral (towards 5) direction resulting in a “fused” QRS VT morphology not reproducible by pacing at either site. Indeed, ablation at the presumed isthmus site (and predicted site of origin), indicated by the white tag, abolished VT.

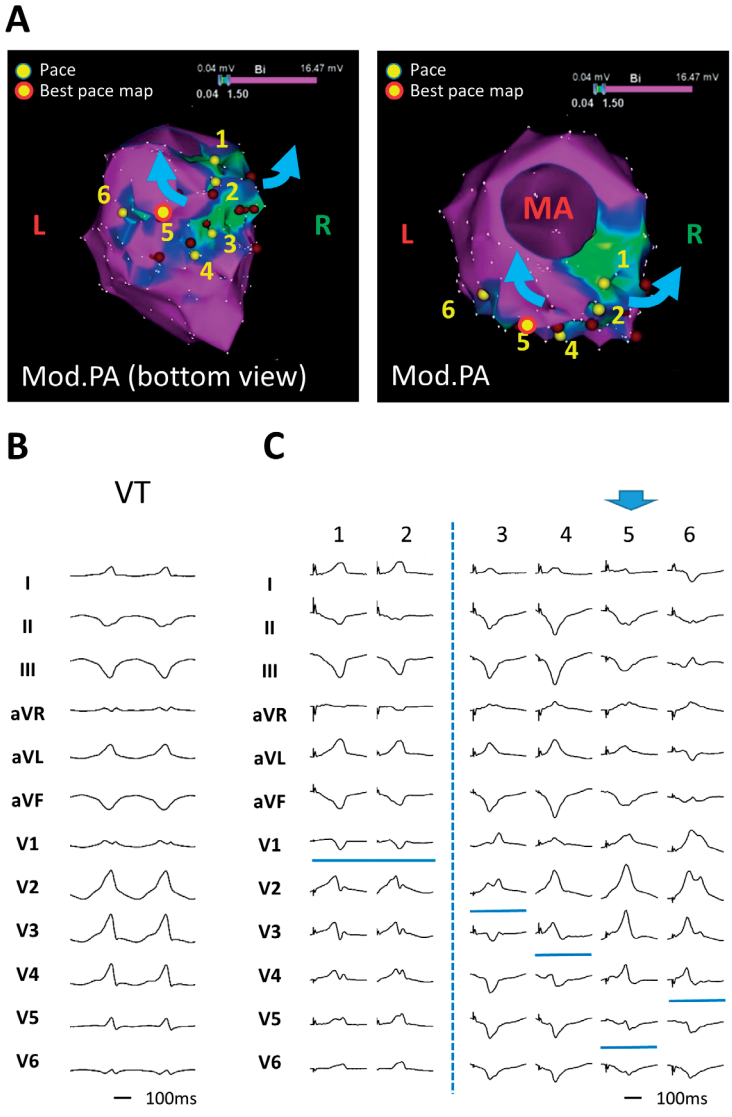
A
Pace
Best pace map
0.04 mV
Bi
16.47 mV
0.04
1.50
1
2
3
4
5
6
L
R
Mod.PA (bottom view)
Pace
Best pace map
0.04 mV
Bi
16.47 mV
0.04
1.50
MA
L
R
1
2
3
4
5
6
Mod.PA
B
VT
I
II
III
aVR
aVL
aVF
V1
V2
V3
V4
V5
V6
100ms
C
1
2
3
4
5
6
I
II
III
aVR
aVL
aVF
V1
V2
V3
V4
V5
V6
100ms

SUPPLEMENTARY CASE 4

69 years male, 17 years after small apical MI, clinical VTCL 375ms

Panel A. EA endocardial bipolar voltage map of the LV in modified anterior (AP), LAO and inferior views (color coded according to the bar) showing a very small dense apicoseptal scar with only little lateral involvement. Grey tags indicate sites with no capture at high output pacing.

The clinical VT (panel C) had RBBB morphology with early precordial transition and right superior axis and a predicted posterior-apical SoO by Segal[6] (not predictable by Miller[4] and Kuchar[5]).

The best pace-map was obtained at site 5 (corresponding catheter position using a transeptal approach on fluoroscopy provided in panel B, red arrows) and ablation adjacent to this point successfully terminated VT.

Please note that pacing at all scar border zone sites resulted in a RBBB morphology with early transition and a superior axis similar to VT (R/S transition is indicated as blue lines). The superior axis can be explained by an inferior-anterior activation of the normal myocardium from all scar border sites. However, subtle QRS axis changes from RS to LS as pacing sites move from right to left (best visible in lead aVL) can direct to the VT scar exit in small apical scars.

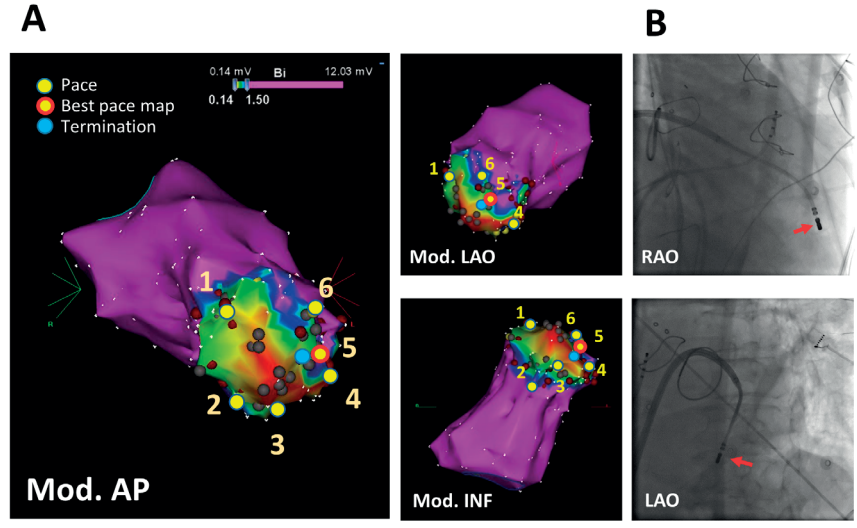
A
B
Pace
Best pace map
Termination
0.14 mV
Bi
12.03 mV
0.14
1.50
Mod. AP
Mod. LAO
Mod. INF
RAO
LAO
1
2
3
4
5
6

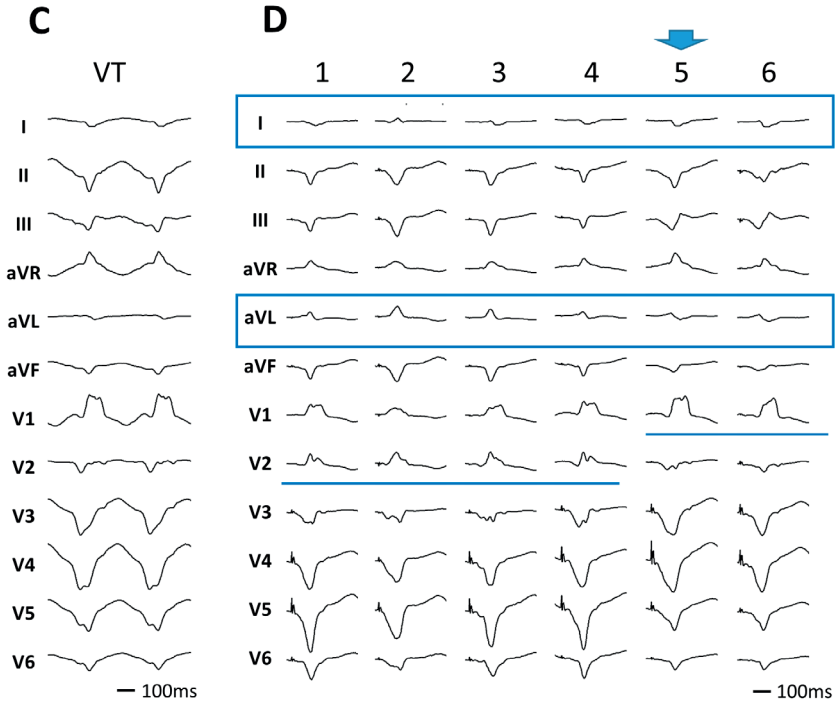
C
D
VT
1
2
3
4
5
6
I
II
III
aVR
aVL
aVF
V1
V2
V3
V4
V5
V6
100ms
100ms

Figure 1

SUPPLEMENTARY CASE 5

64 years male, 16 years after large anterior MI, clinical VTCL 440ms

Panel A. EA endocardial bipolar voltage map of the LV in modified RAO and LAO views (color coded according to the bar, grey tags indicate sites with no capture at high output pacing). Tags represent catheter positions as indicated; numbers correspond to the numbers of the paced 12 lead ECG morphologies (Panel C).

The clinical VT (panel C) had RBBB morphology with positive concordance and left inferior axis, which was rarely observed in Miller's[4] report (2 out of 78 RBBB VT from anterior infarctions) but had a predictable anterobasal SoO according to Kuchar[5] and Segal[6]. The best pace-map was obtained at the basal anterior EA scar border (site 2). Please note the abrupt change in the paced QRS morphology from a left inferior axis to a left superior axis with early precordial transition if pacing moved from the basoseptal EA scar border zone (site 1, corresponding catheter position on fluoroscopy, panel B, red arrows) to the mid-septal (site 3) border zone. The EA scar extension (dashed line, panel A) between these two sites may lead to different propagation wave fronts and abrupt changes in the paced QRS morphology. Please also note that pacing at mid anteroseptal sites (point 3 and 4) resulted in a RBBB morphology with early transition with left superior axis while pacing at mid lateral sites (point 9 and 10) had later transition and less superior axis. Unexpected ECG morphologies are likely related to the variation in scar distribution after anterior MI and may explain the limited predictive value of prior algorithms.

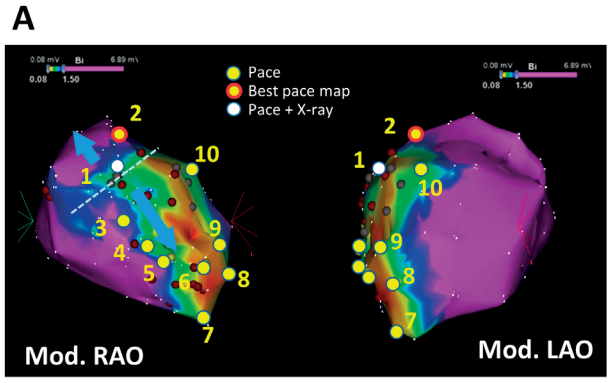
A
Pace
Best pace map
Pace + X-ray
Mod. RAO
Mod. LAO
B
RAO
LAO
C
D
VT
Pace mapping
1
2
3
4
5
6
7
8
9
10
I
II
III
aVR
aVL
aVF
V1
V2
V3
V4
V5
V6
100 ms

Figure 5

SUPPLEMENTARY CASE 6

73 years male, 16 years after inferolateral MI, epicardial ablation after endocardial ablation failure, clinical VTCL 630ms

Panel A. EA endocardial bipolar voltage map of the LV in modified left lateral and posterior views (color coded according to the bar, grey tags indicate sites with no capture at high output pacing). Tags represent catheter positions as indicated; position of the best endocardial pace-map on fluoroscopy in RAO and LAO view (red arrows). Numbers correspond to the numbers of the paced 12 lead ECG morphologies (Panel D).

Panel B. EA epicardial bipolar voltage map of the LV in the same modified left lateral and posterior views as panel A (color coded according to the bar, please note that for the epicardium, a bipolar cut off <1.8mV for abnormal voltage is applied[14], grey tags indicate sites with no capture at high output pacing). Tags represent catheter positions as indicated; position of the best epicardial pace-map after endocardial ablation failure on fluoroscopy in RAO and LAO view (red arrows). Numbers correspond to the numbers of the paced 12 lead ECG morphologies (Panel E).

The clinical VT had RBBB morphology, positive concordance, inferior axis, not classifiable by Miller[4] and with a predicted mid to basal anterior SoO according to Kuchar[5] and Segal[6] (panel C, left). The best, although not perfect endocardial pace-map was obtained at endocardial site 1 (panel A, D). After RF at the endocardium a similar VT remained inducible (VT´) with slightly shorter CL and subtle changes of the initial part of the VT QRS (panel C, right) suggesting an epicardial exit site.

ECG criteria for a potential epicardial site of origin (sweep speed 100mm/sec) were applied; Pseudodelta wave (PDW ≥ 34ms), Intrinsicoid deflection time inV2 (IDT ≥ 85), Shortest RS complex (SRS ≥ 121ms), Maximum deflection index (MDI ≥ 0.45). Despite a similar morphology, after endocardial ablation VT´ QRS was broader (251ms vs. 387ms after) and ECG parameters were strongly suggestive for an epicardial origin; PDW 65ms vs 198ms, IDT 112ms vs 252ms, SRS 182ms vs 322ms and MDI 0.39 vs 0.59 in VT before and after endocardial ablation. Notably, morphology criteria did not differentiate between endo and epicardial pacing sites (Q-waves), perhaps because of the transmural lateral scar.

During epicardial mapping, the best pace-map for VT´ could be obtained at epicardial site 1 (epicardial catheter position on fluoroscopy opposite (slightly lateral) to the endocardial catheter position). With the catheter in place VT was re-induced and terminated

after 6 seconds RF. The change in QRS morphology after endocardial ablation may be explained by a shift in exit site from the endocardium to the epicardium.

Voltage mapping showed a remarkable anterior scar extension, which explains the unusual 12 lead VT QRS morphology in a patient after inferolateral MI.

Please also note the abrupt change in the precordial leads between pacing site 4 and 5 from a RS in V1, negative concordant in the precordial leads to a RBBB, late transition morphology. These changes may be explained by the scar extension and transmurality as derived from endo and epicardial voltage mapping resulting in different wavefront propagation and QRS morphologies.

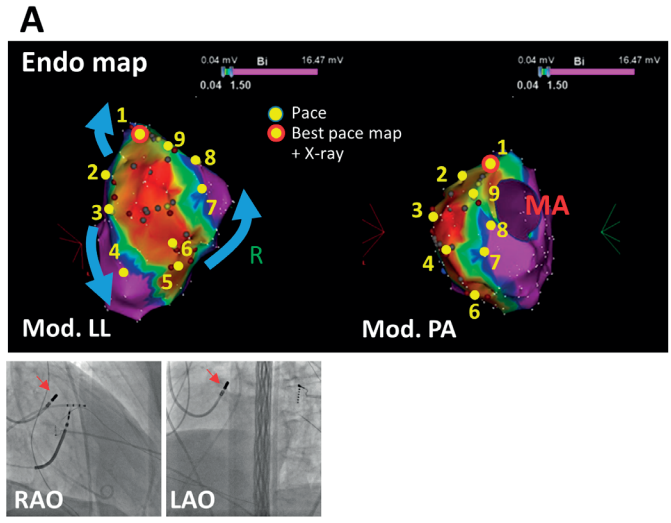
A
Endo map
0.04 mV
Bi
16.47 mV
0.04 1.50
Pace
Best pace map
+ X-ray
MA
R
Mod. LL
Mod. PA
RAO
LAO

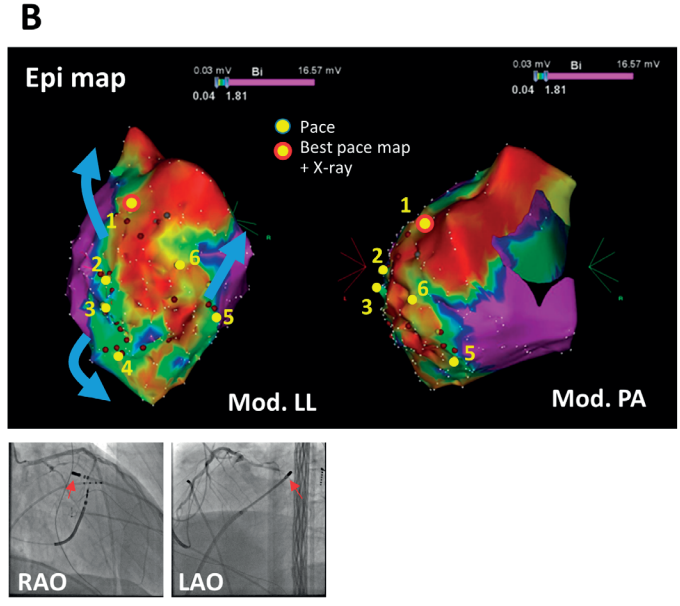
B
Epi map
0.03 mV
Bi
16.57 mV
0.04 1.81
Pace
Best pace map
+ X-ray
Mod. LL
Mod. PA
RAO
LAO

SUPPLEMENTARY CASE 7

62 years male, NICM, clinical VTCL 405ms

Panel A. EA endocardial bipolar voltage map of the LV in modified RAO and LAO views, the aorta (Ao) and the RV (modified RAO and posterior view[LV transparent]) (color coded according to the bar, grey tags indicate sites with no capture at high output pacing). Tags represent catheter positions as indicated; numbers correspond to the numbers of the paced 12 lead ECG morphologies (Panel D).

Panel B. EA epicardial bipolar voltage map in a modified LAO view (left) and integration of the CT derived anatomy of the aorta, left atrium and coronary arteries (LAD, left anterior descending coronary artery) with the endocardial EA maps (right, same modified LAO view).

The endocardial EA scar was confined to the basal anteroseptal LV, which is one of the typical scar patterns observed in NICM patients[27]. Image integration demonstrates that this particular area is not reachable from the epicardium. The epicardial low voltage area (ventricular electrograms annotated) is covered by the large left atrial appendage (LAA) and the fat overlying the LAD at the interventricular groove.

The clinical VT (Panel C, 50mm/sec [left]; 100mm/sec [right]) had a RBBB morphology with positive concordance and right inferior axis, suggesting an origin from the antero-basal LV, so called 'LV summit'. ECG parameters were indicative of an epicardial SoO (PDW 135ms (≥34ms), IDT 275ms (≥ 85), SRS 270ms (≥ 121ms) and MDI 0.56 (≥ 0.45)). The best although not perfect pace-map (no prolonged initial slurring in precordial lead V3) was obtained just beneath the aortic valve (panel D, endocardial site 7). Ablation at the endocardial LV basal anterolateral region could modify but not abolish the VT. Pace mapping neither at RV, CS or aortic cusp sites could resemble VT QRS. Although epicardial mapping was performed, neither pace-mapping nor activation mapping could identify a VT related site. Although no complication related to the epicardial access occurred in this patient, the 12 lead VT ECG morphology combined with the information from image integration after endocardial substrate mapping can predict a VT substrate not accessible from the epicardium.

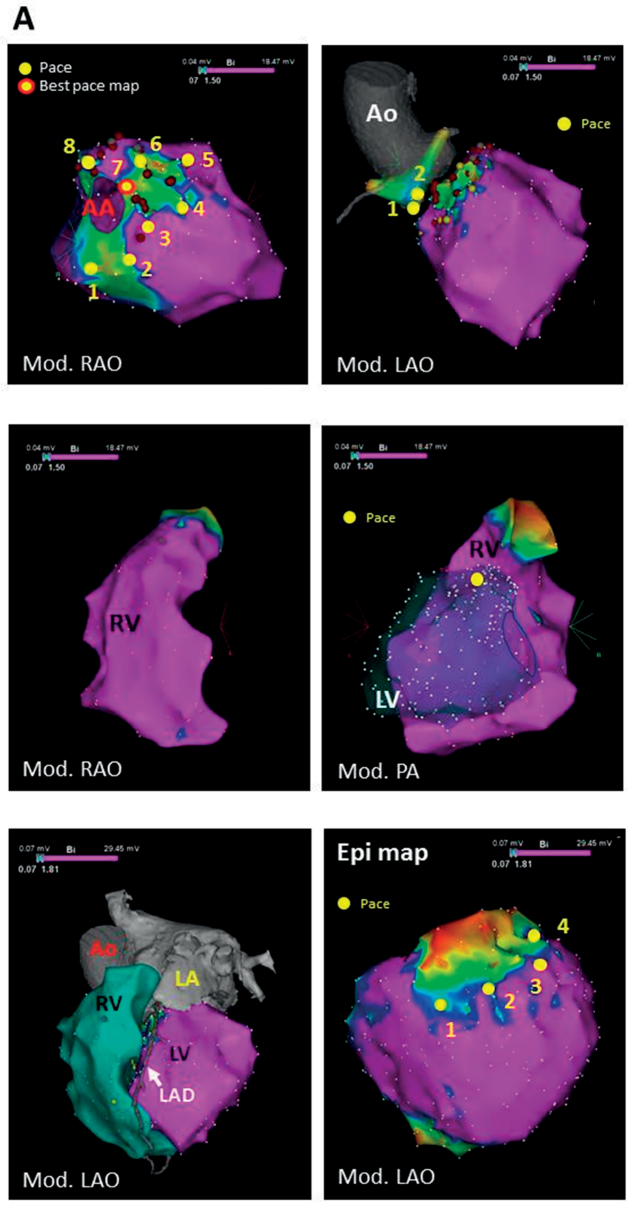
A
Pace
Best pace map
8
7
6
5
AA
4
3
2
1
Mod. RAO
Ao
Pace
2
1
Mod. LAO
RV
Mod. RAO
Pace
RV
LV
Mod. PA
Ao
LA
RV
LV
LAD
Mod. LAO
Epi map
Pace
4
3
2
1
Mod. LAO

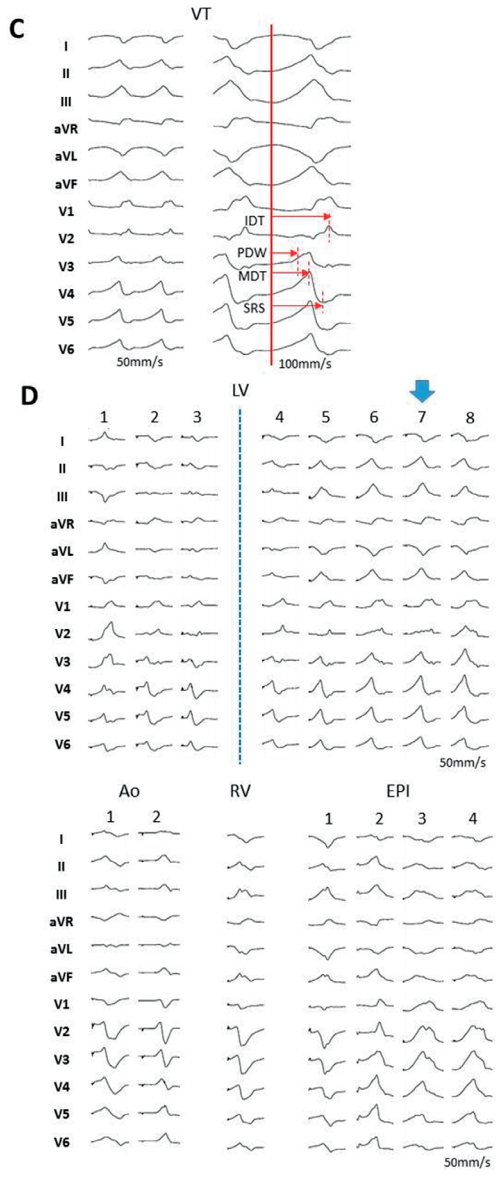
C
VT
I
II
III
aVR
aVL
aVF
V1
V2
V3
V4
V5
V6
IDT
PDW
MDT
SRS
50mm/s
100mm/s
D
LV
1 2 3 4 5 6 7 8
50mm/s
Ao
RV
EPI
1 2
1 2 3 4
50mm/s